Journal of Innovative Optical Health Sciences
Vol. 13, No. 2 (2020) 2030003 (12 pages)

DOI: 10.1142/S1793545820300037

Review of methods to improve the performance of linear array-based photoacoustic tomography

Yuehang Wang, Ye Zhan, Melinda Tiao and Jun Xia*
Department of Biomedical Engineering
University at Buffalo, State University of New York
Buffalo, NY 14260, USA
**junxia@buffalo.edu*

Received 23 September 2019
Accepted 10 November 2019
Published 6 December 2019

As a hybrid imaging modality that combines optical excitation with acoustic detection, photoacoustic tomography (PAT) has become one of the fastest growing biomedical imaging modalities. Among various types of transducer arrays used in a PAT system configuration, the linear array is the most commonly utilized due to its convenience and low-cost. Although linear array-based PAT has been quickly developed within the recent decade, there are still two major challenges that impair the overall performance of the PAT imaging system. The first challenge is that the three-dimensional (3D) imaging capability of a linear array is limited due to its poor elevational resolution. The other challenge is that the geometrical shape of the linear array constrains light illumination. To date, substantial efforts have been made to address the aforementioned challenges. This review will present current technologies for improving the elevation resolution and light delivery of linear array-based PAT systems.

Keywords: Photoacoustic tomography; linear array ultrasound transducer; spatial resolution.

1. Introduction

Photoacoustic tomography (PAT) is a promising biomedical imaging modality that offers high-resolution optical absorption imaging of deep tissue. The hybrid acoustic detection of optical absorption overcomes the optical diffusion limitation.[1–5] PAT forms images based on the photoacoustic (PA) effect, which was first discovered by Alexander Bell more than 100 years ago. The research for photoacoustic imaging (PAI) developed very slowly until the 1990s. At this time, the development of high-power pulsed lasers, sensitive ultrasonic transducers, and data acquisition systems triggered the rapid development of PAI. Since then, the technique has evolved rapidly and became one of the most exciting biomedical imaging techniques in this decade. In the last few years, PAT has been demonstrated in various preclinical and clinical

*Corresponding author.

applications, such as cardiology imaging,[6] oncology imaging,[7] vascular biometrics,[8] functional imaging,[9–12] breast cancer screening,[13,14] and guidance of lymph node biopsy.[15]

In terms of acoustic signal detection configuration, various ultrasonic transducer arrays, such as ring array,[16,17] linear array,[18–22] and hemispheric array,[13,14] have been implemented in the PAT system to meet the demand of preclinical and clinical applications. Among these, linear transducer arrays are probably the most widely used. As the name implies, the piezoelectric elements of the linear transducer array are arranged in a line, thus, producing a rectangular field of view. Compared to other arrays, linear arrays are handheld operable, convenient, and very affordable. It can be easily manufactured and integrated with light sources and conventional ultrasound systems.

Although linear array-based PAT is promising and has been quickly developed, it still faces challenges that impair the imaging performance of the system. The spatial resolution of a linear transducer array can be represented in three axes. Within the imaging plane shown in Fig. 1(a), the axial direction is along the axis that is perpendicular to the transducer element surface, and the lateral direction is perpendicular to the axial direction. The elevational direction is orthogonal to the rectangular imaging plane.

In a linear array-based PAT, the axial resolution (Fig. 1(a)) is primarily defined by the center frequency of the transducer, while the lateral resolution (Fig. 1(a)) is determined by the element pitch of the array. Typically, the axial resolution equals half of the central acoustic wavelength, while the lateral resolution equals one central acoustic wavelength.[5]

Along the elevation direction, the elements of the linear array transducers are usually cylindrically focused to achieve a cross-sectional imaging plane (Fig. 1(a)). For 3D PAI, the volumetric image can be obtained by stacking two-dimensional (2D) images. In this case, the linear transducer array has to be scanned along the elevation direction. However, because of the fixed cylindrical focus, the resulting volumetric images have a poor spatial resolution along the scanning axis. As shown in Fig. 1(a), the elevation resolution is the highest at the acoustic focus, and it degrades as the object moves away from the focus. Even at the elevational focus, both the axial and lateral resolutions are better than the elevational resolution by at least three times.[5,23,24]

Besides the nonisotropic spatial resolution, the arrangement of the linear elements limits the light delivery to the image plane of the linear array-based PAT systems. Since the image plane is right under the elements' surface, the light can only be delivered from the side of the probe for most linear array-based PAT systems (Fig. 1(b)). The side illumination creates additional challenges because it is hard to control the light incident angle according to the distance/depth of the object.

Over the past few years, numerous researchers have made substantial efforts to address these limitations. In this review, current technologies to improve elevation resolution and light delivery of the linear array-based PAT will be presented.

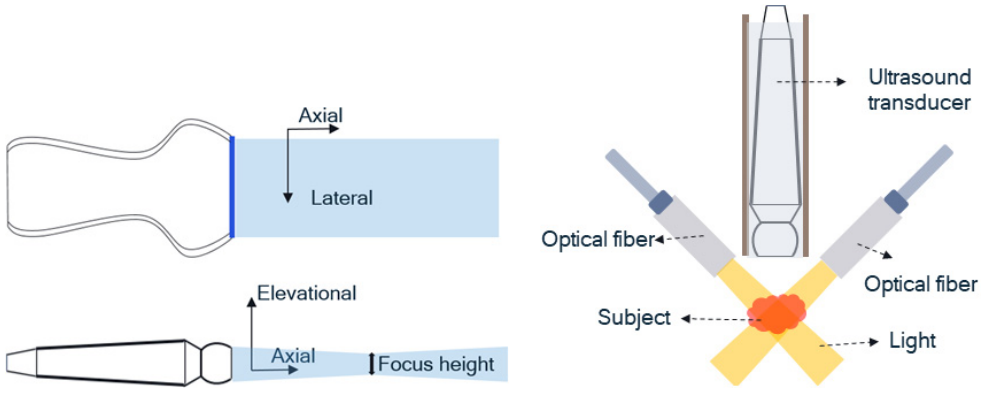

(a) (b)

Fig. 1. Schematic drawing of a linear array transducer. (a) Top: Imaging plane of the linear array transducer. Bottom: Side view of the focal zone of the linear array transducer. (b) Light delivery scheme for side-illumination PAI.

2. The Principle of PAT

Before talking about the details of each system, we first introduce the principle of PAT (Fig. 2).

PA signals are typically generated by shorted-pulsed lasers. Upon laser irradiation, the object will absorb the photon energy and experience transient thermos-elastic expansion, resulting in the generation of wideband ultrasound signals. For an effective ultrasound signal generation, the pulse duration is typically within a few nanoseconds, which is lower than both the thermal and stress confinements.[25] After the wideband emission, the induced acoustic waves are then detected by ultrasound transducers. Finally, the distribution of optical absorption can be obtained by performing an image reconstruction of the detected signals. The PA pressure (p_0) can be written as the following equation:

$$p_0(\vec{r}) = \Gamma \mu_a F(\vec{r}),$$

where Γ is the Grueneisen parameter which increases linearly with temperature, μ_a is the absorption coefficient, and $F(\vec{r})$ is the local optical fluence.

The sound pressure propagates to the tissue surface at different time delays due to the various location of the sound source and properties of the tissue. Linear array-based PAT uses an array of ultrasound transducers to record the sound waves. The distribution of the initial sound pressure or electromagnetic absorption can be obtained by inversely projecting back the detected sound waves. There are many approaches for PAT imaging reconstruction. Among them, the time-domain back-projection reconstruction algorithms are probably the more widely used.[26] These methods assume a homogeneous acoustic property in tissue, and the speed of sound in the soft tissue is relatively constant at around 1.5 mm/ μs.[27]

3. Technologies for Improving the Elevation Resolution

To improve the elevational resolution of linear array-based PAT, researchers have proposed numerous solutions. They include new scanning geometries, new detection hardware designs, and advanced image reconstruction algorithms.

3.1. *Modifying the scanning geometries to improve the elevation resolution*

Gateau *et al.* first investigated a novel scanning geometry that combined linear and rotational scanning to achieve nearly isotropic 3D spatial resolution.[28] As shown in Fig. 3(a), the proposed geometry employs two movements of the linear array, including translation and rotation. The linear array was perpendicularly mounted on a linear translation stage, which was further fixed on a rotary stepper motor so that the stage could be rotated. The entire scanning setup was moved to discrete positions along the contour of a polygon. Each of the translation ranges (polygon sides) was 13.5 mm and tangent to a circle centered on the axis of rotation. The entire rotation range was 180°. A 128-element linear array (5.0/7.0 MHz, Acuson L7, Siemens) was used to test this method. The spatial resolution of the PAT system was measured through imaging 50 mm diameter microspheres. The resulting spatial resolutions were 130 μm in-plane and 330 μm in elevation.

Upon the initial study of the combined linear and rotational scanning geometry, Gateau *et al.* proposed a novel single-sided access rotate-translate linear array-based PAT scanner.[29] In this system, a 128-element linear array (Vermon, Tours, France) with a 15 MHz center frequency, 101 μm element pitch, and 1.5 mm cylindrical focus was applied. A motorized translation stage and goniometer stage

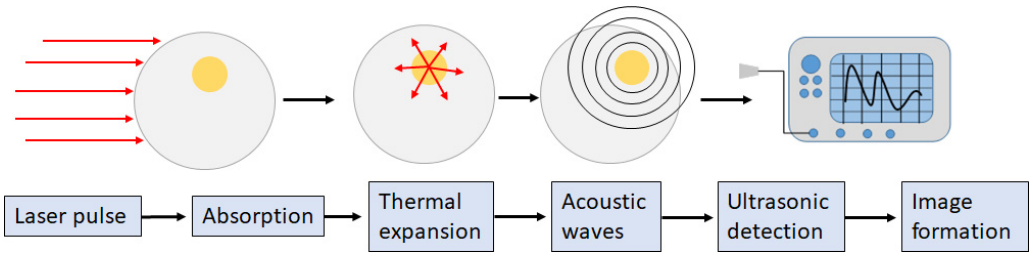

Fig. 2. Principle of PAI.

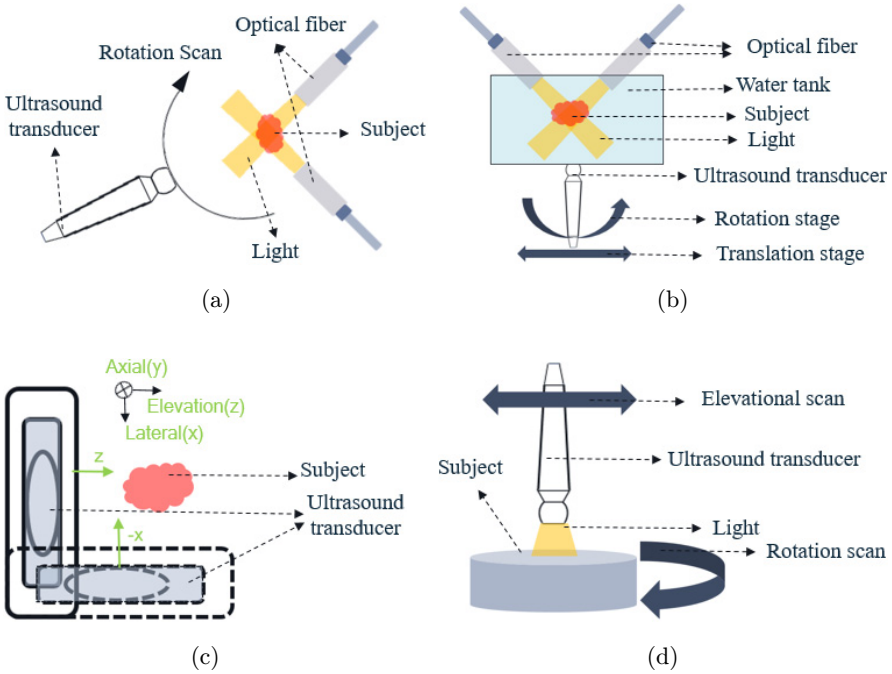

Fig. 3. Different scanning geometries for improving elevation resolution. (a) The rotational scanning geometry proposed in Ref. 28. (b) The translate-tilting scanning geometry proposed in Ref. 29. (c) The bi-directional scanning geometry proposed in Ref. 30. (d) The sample-rotational scanning geometry proposed in Ref. 31.

were used to combine translation and rotation motions. The maximum travel range was 50 mm for the translation stage and 90° for the rotation stage. As shown in Fig. 3(b), the linear transducer array was mounted on the goniometer stage and then translated by the translation stage. To ensure that the motion of the elements' centers was within the XY-plane, the length axis of the linear array was mechanically aligned to match the rotation axis of the goniometer. During the scanning, the array was continuously and simultaneously translated and rotated from −45° to 45°. Similar to their initial study, microspheres phantom was used to test the spatial resolution of the PAT system. The spatial resolution results show that the proposed system has a quasi-isotropic 3D resolution of ∼170 μm. The improvement of spatial resolution in the translation direction is almost one order of magnitude.

Besides the translate-rotate scanning geometry, Schwarz *et al.* proposed a bi-directional scan method with two array positions perpendicular to each other to improve the elevation resolution.[30] As shown in Fig. 3(c), two linear scans were conducted in perpendicular directions (x- and z-direction) for bi-directional scanning. A 24 MHz 128 element linear transducer array (LA28.0/128, Vermon, Tours, France) with a 1.5 mm focus and 70 μm pitch was first scanned along the elevation direction and was then rotated by 90° and scanned across the same region again. Numerical simulation and experimental phantom resolution studies both demonstrated that the method yields an improved elevation resolution with only minor losses in lateral resolution.

Li *et al.* also proposed a combined linear and rotational scanning method to achieve isotropic resolutions for linear array-based PAT.[31] Instead of rotating or translating the array over the sample, a rotating sample and translational scanned linear array were adopted, as shown in Fig. 3(d). In each scan step, a commercial linear array with 256 elements (LZ250, 21 MHz center frequency, Visualsonics Inc., Canada) was first elevationally scanned. Then the sample was rotated around its center in a 2° angular step size and scanned again until 180° have been covered. Carbon fiber was chosen to quantify the elevation resolution of the proposed system, and the resolution result shows that this method improves the elevational resolution by 10 times in comparison with the conventional single elevational scan.

In principle, the various scanning geometries discussed above improve elevation resolution by converting the elevation direction into axial or

lateral directions. This conversion overcomes the intrinsic limitation of the linear array transducer. However, such complicated scanning geometry often means a prolonged scanning time. The large data size also takes more time to process for image reconstruction.

3.2. *Modifying the detection scheme to improve the elevation resolution*

Without modifying the scanning geometry, Wang *et al.* proposed a fundamentally different approach to improve elevation resolution. The technique is based on acoustic diffraction through a thin slit, which essentially improves the receiving angle of the array along the elevation direction (Fig. 4).[32] The imaging system exploited an ATL/Philips L7-4 128-element linear transducer array (5 MHz center frequency, 25 mm elevation focus) and a thin slit formed by two metal blades with 500 μm thickness. The bottom blade was fixed in position while the top blade was mounted on a translation stage, allowing for easy and precise control of the slit opening (from 300 μm to 1000 μm). The thin slit diffracts the incoming PA waves along the elevation direction and enables 3D image reconstruction. Through phantom and *in vivo* experiments, the authors demonstrated that the slit improves the elevation resolution by up to 10 times without compromising scanning time.[31] Besides improvement in elevation resolution, the slit also improves the signal-to-noise ratio (SNR) due to a larger receiving aperture. Figure 4 displays the vascular image results of a human palm acquired by slit-based linear PAT.

3.3. *Imaging algorithms for improving the elevation resolution*

Other than modifying the system hardware, advanced imaging algorithms can also improve the elevation resolution of the linear array-based PAT system. Wang *et al.* proposed the integration of two advanced image reconstruction techniques: coherent weighting (CW) and focal-line (FL) 3D image reconstruction.[34,35]

The CW algorithm calculates the coherence of received PA signals and assigns a weighting factor to the delay-and-summed signals. The value of the coherent weighting factor (CWF) ranges from 0 to 1 and can be applied to the reconstructed image. This factor enhances the coherently summated signals while suppressing the out-of-phase signals and randomized noise. The CW factor is applied in 3D through the FL reconstruction algorithm, which precisely calculates the time of arrival in 3D space. Previous studies have indicated that the FL algorithm can improve the elevation spatial resolution up to the size of the acoustic focus (Fig. 1(b)) regardless of the axial distance of the object.[34] The combined CW–FL algorithm was validated through numerical simulation and was experimentally tested in both phantom and human subjects. Both of the experiments' results proved that the method can significantly improve the elevation resolution by 4 times; moreover, the method also suppresses noise and offers higher SNR.

Alshaya *et al.* reported another algorithm named the[36] Filter Delay Multiply and Sum (FDMAS) beamforming technique, which is an adaptive beamforming technique that depends on the

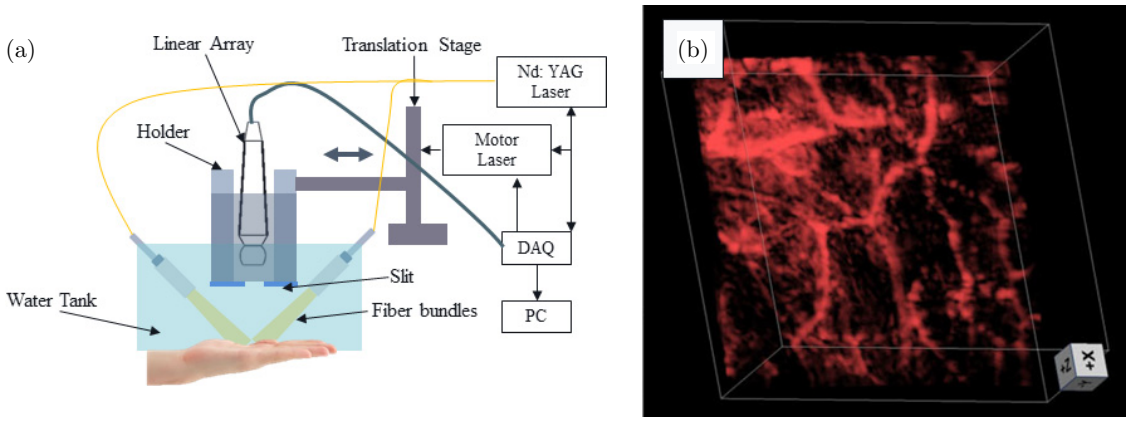

Fig. 4. Slit-based linear PAT proposed in Ref. 33. (a) Schematic drawing of the slit-based linear-array PAT system. (b) 3D palm vascular images acquired by the slit technology. This work by Y. Wang *et al.*, Ref. 33 is licensed under a Creative Commons Attribution 4.0 International License.

Table 1. Comparison of different methods for improving the elevation resolution in a linear array.[35] The table was reproduced with permission from Ref. 35.

Name	Scanning method	Speed	Modification of transducer array	Improvement in elevation resolution
Rotational scanning geometry[38]	180° rotational scan +translational scan at each 1.5° interval	Slow	No	High
Translate-tilting scanning geometry[29]	Continuous and simultaneous rotation and translation scan	Slow	No	High
Bi-direction scanning geometry[30]	Two translational scans perpendicular to each other	Medium	No	Medium
Sample-rotational scanning geometry[31]	The sample is rotated in increments and linearly scanned	Slow	No	Medium
Slit PAT geometry[32]	One translational scan	Fast	Yes (slit)	High
CW–FL[35]	One translational scan	Fast	No	Medium
FDMAS[36]	One translational scan	Fast	No	Medium

autocorrelation between delayed radio frequency (RF) data. Due to the autocorrelation operation, the FDMAS beamforming technique cannot be applied directly in 3D PAI. Instead, the FDMAS is used to beamform the RF data in the lateral direction and elevation direction separately, and then combine them. This FDMAS beamforming technique not only improved the elevation resolution out of the focal length, but also reduced the clutter signals and background noise of the PA image. The FDMAS beamforming technique was compared with the Delay and Sum (DAS) beamforming technique in terms of spatial resolution and SNR. The improvement in the elevation resolution and SNR are about 30% and 13 dB compared to DAS, respectively.

Table 1 summarizes different techniques used to improve the elevation resolution.[37] It can be seen that the last three methods possess the fastest speed because they require only a single translational scan, while the first two methods provide the best improvement in elevation resolution because they translate the elevation direction into axial direction during the scan. The middle two methods convert elevation direction into lateral direction during the scan. Depending on the scanning method, the speed ranges from medium to slow.

4. Technologies for Improving Light Delivery Efficiency

Due to the linear arrangement and cylindrical focus of the array elements, the imaging plane of linear array transducers is a cross-sectional plane that extended along the axial direction. As we introduced in Sec. 2, the intensity of the PA signal primarily depends on the local light fluence and absorption coefficient. To achieve optimal PAI depth, we need to ensure that the majority of light goes to the imaging plane. In this case, coplanar light delivery and acoustic detection would be the optimal geometry. In reality, due to the geometric shape of linear array transducers, the light is typically delivered from the side of the linear array. Because of the noncoaxial light delivery and acoustic detection, a good amount of the light energy will be wasted outside of the imaging plane. The large incident angle also increases the light travel distance. Both efforts lead to a shallower imaging depth in side-illumination PAT systems. This conclusion is supported by Monte Carlo simulations,[39,40] which found that smaller incident angles could significantly improve the light fluence in deep imaging regions.

In this section, we will first discuss technologies for improving the efficiency of side illumination, and then introduce methods to achieve coplanar (coaxial) light delivery and acoustic detection.

4.1. *Adjustable side light delivery*

Liu *et al.* designed and built a handheld, real-time PAI system with manually adjustable side light delivery.[41] To optimize the laser light delivery, a finite element simulation was employed to evaluate the influence of the incident angle and interval

between the two arms of the fiber bundle regarding light fluence. Phantom experimental validations were performed and the results were consistent with the simulations results. These results indicated that the distance between the two arms of the fiber bundle played a major role in light fluence propagation.

Besides the manual adjustment, Sangha *et al.* reported a motorized adjustable PAT probe.[42] The adjustable PAT holder (Fig. 5) consists of an external linear stepper motor and two bipolar stepper motors. This holder can vertically translate the ultrasound transducer and adjust the fiber bundle's rotation and angle. These adjustments could improve the optical fluence of different tissue layers, thereby increasing the penetration depth and SNR. By tuning the fiber orientation, probe-skin reflection artifacts were reduced and light distribution in the image acquisition plane was improved. They validated the motorized PAT probe through Monte Carlo simulations, *ex vivo* imaging, and *in vivo* imaging. The *ex vivo* results showed several millimeter improvements in penetration depth, while the *in vivo* results showed a 62% increase in lipid SNR.

4.2. *Coaxial light delivery and acoustic detection*

Although side light delivery is widely used in linear array-based PAT systems, coaxial light delivery and acoustic detection is still the optimal light delivery method. The first coaxial system was proposed by Montilla *et al.*, who utilized an optically transparent acoustic reflector to separate light illumination and acoustic detection into two directions.[43] As shown in Fig. 6, the glass plate is transparent to light while the acoustic waves were reflected by 90°, achieving coaxial illumination and detection. The performance of the system was demonstrated by imaging a mouse with a pancreatic tumor.

Lee *et al.* proposed a handheld probe in which the illuminated light beam axis coincides with the axis of the ultrasound through a beam combiner.[44] The beam combiner doubly reflects the acoustic waves to the linear array transducer and the transmission losses of the light and acoustic beams are low. Moreover, the laser output was shaped to a line beam by three cylindrical lenses (Fig. 7). In their small animal experiments, the lymph nodes near the skin could be detected without the need for any supplementary material.[44]

Li *et al.* proposed a similar handheld probe design, utilizing polymethyl methacrylate (PMMA) as an optical/acoustic coupler.[27] The optical/acoustic coupler reflects the light beam two times and is permeable to acoustic waves, achieving coaxial light delivery and acoustic detection with the optical fiber bundle and transducer probe parallel to each other. Using the handheld probe, the authors successfully imaged the sentinel lymph node (SLN) in a live rat. Li's group has also designed various types of compact PA probes to improve the SNR of the system[45] and to detect the SLN.[46]

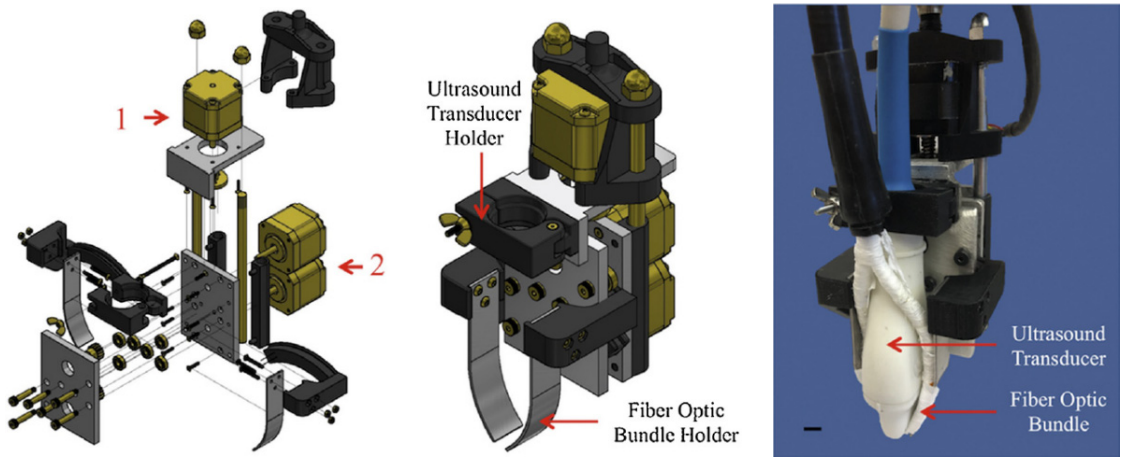

(a) (b) (c)

Fig. 5. The adjustable probe proposed in Ref. 42. Exploded (a), presentation (b), and constructed (c) images of the probe. Reprinted from Photoacoustics, 12, G. S. Sangha, N. J. Hale, C. J. Goergen, Adjustable photoacoustic tomography probe improves light delivery and image quality, 6–13., Copyright (2018), with permission from Elsevier.

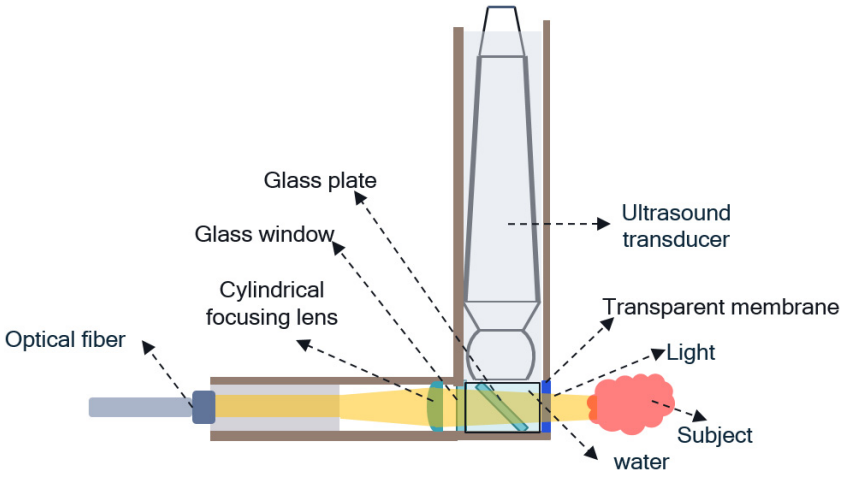

Fig. 6. Cross-sectional view of the photoacoustic enabling device (PED) design.[43] In this design, a glass plate was used as a light and sound combiner.

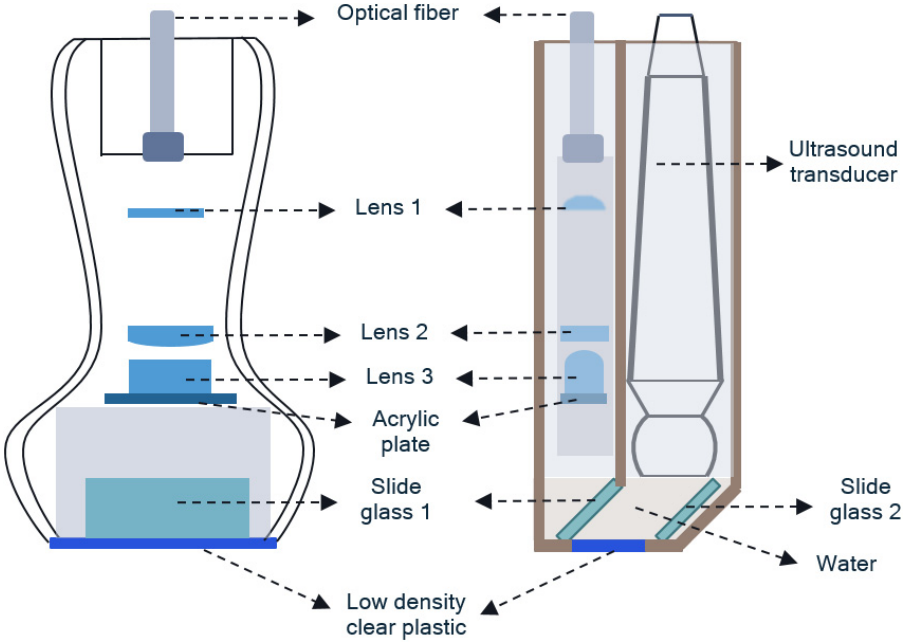

Fig. 7. Schemes of a handheld probe with the illuminated light beam axis coincides with the axis of the ultrasound through a beam combiner.[44]

Recently, Wang *et al.*[47] reported another double-reflector design-based linear optical fiber bundle. Instead of the optics shown in Fig. 7, their system utilized a line output fiber bundle to illuminate the object, so that the whole system is much easier to align. In this design, a compact housing was created to combine both the transducer and fiber bundle output for convenient handheld imaging (Fig. 8). Various phantom and human *in vivo* experiments were performed to evaluate the efficiency of the system. 3D vascular images of the human forearm were acquired as shown in Figs. 8(b) and 8(c). The images demonstrated that the double-reflector design provides a deeper imaging depth than that of side illumination.

Table 2 compares different light illumination schemes. It can be seen that while the side illumination is easy to implement, it has limited light penetration depth. The single-reflector design achieves coplanar light illumination and acoustic

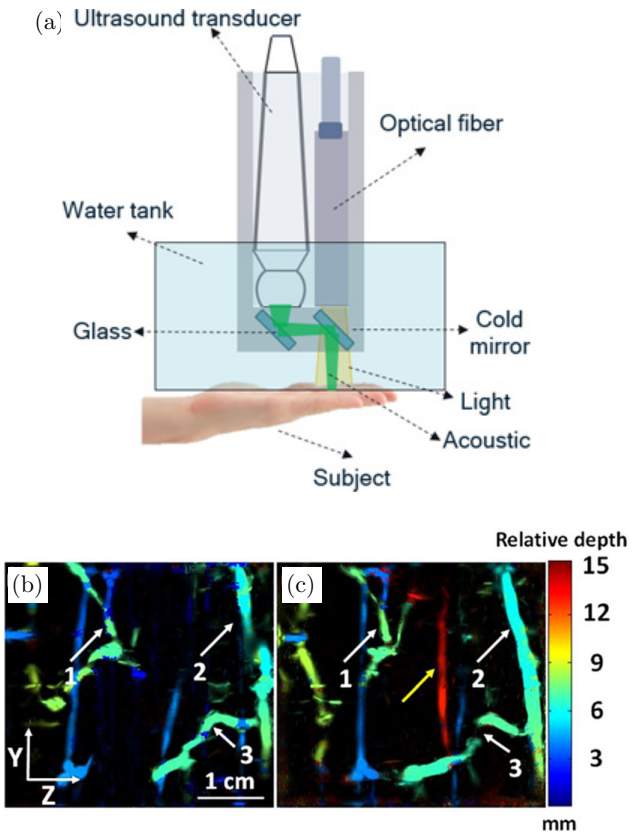

Fig. 8. Schemes of a Double-reflector PAI system.[47] (a) The cold mirror is transparent to the near-infrared light, while it reflects acoustic waves by 90°. The second acoustic reflection was achieved by a regular glass. (b) Depth-encoded Maximum amplitude projection (MAP) image of a human forearm, acquired by the side-illumination system. (c) Depth-encoded MAP image of the forearm, acquired by the double-reflector system. White arrows show the same features and the yellow arrow indicates the deepest vessel. This work by Y. Wang *et al.*, Ref. 47 is licensed under a Creative Commons Attribution 4.0 International License.

detection with the minimal wave aberration, however, it is inconvenient for handheld operation. The double-reflector system represents the most compact design among the three. However, it is also associated with a longer acoustic travel distance, which needs to be considered during image reconstruction.[47]

5. Summary and Conclusions

Linear array-based PAT is a high resolution, non-invasive, and convenient imaging modality with extensive applications from preclinical laboratory research to clinical patient care. However, due to the unique geometry design of the linear transducer array, it still faces engineering challenges in terms of poor elevation resolution and light delivery that would impair the imaging performance of the PAT system. In this review, we discussed the state-of-the-art of linear array-based PAT systems, introduced the implementation of the imaging system, and elaborated on the reasons for those engineering challenges. We provided a comprehensive review of existing studies and progresses to solve limitations on the elevation resolution and light delivery scheme.

The elevation resolution improvement technologies can be classified into three categories based on their principles. The first category involves new scanning geometries to improve the elevation resolution. Through modified scanning geometries, the elevation direction was converted into axial or lateral directions. However, in consideration of the elongated scanning and imaging reconstruction time, these techniques did not improve the elevation resolution effectively. The second category is based on a brand new technology that improves the elevation resolution by diffracting the acoustic waves through a thin slit. This method provides the highest elevation resolution improvement without modifying the scanning geometry. Furthermore, the slit width can be adjusted to achieve optimal resolution based on the imaging feature. The third category is the simplest method because it improves the elevation resolution purely through imaging

Table 2. Comparison of various light illumination schemes.

Light delivery systems	Advantages	Disadvantages
Side illumination	Easy to implement. Minimal light and acoustic distortion	Limited imaging depth.
Single-reflector illumination	Coplanar light illumination and sound detection.	Inconvenient for handheld operation
Double-reflector illumination	Compact design; Coplanar light illumination and sound detection.	Long acoustic travel distance; potential aberration from two acoustic reflectors.

reconstruction. Although these algorithm-based methods do not require any hardware modification, their elevation resolution improvement is very limited.

As for the light delivery technologies, there are two major solutions: improving the side-illumination design and achieving coaxial light delivery and acoustic detection. To improve the side-illumination design, it is critical to increase the light fluence within the acoustic detection area. For the first solution, linear array-based PAT systems with adjustable light delivery angles were developed to dynamically control the illumination. As for the second solution, the basic principle is to use acoustic and light combiners to separate or combine light and acoustic beams. The coaxial light delivery and acoustic detection technology has been well demonstrated in imaging animal SLNs and human vasculature. All the aforementioned technologies have greatly improved the imaging capability of the linear array-based PAT system.

To further improve the imaging quality, we envision that future studies will combine the elevation resolution improvement techniques and light delivery schemes to achieve both deeper penetration depth and higher spatial resolution in a linear array. With increasing demand in preclinical and clinical applications of PAT, we anticipate that other areas of linear-array PAT, such as light source and data acquisition system, will also be improved to further reduce the system size and detection sensitivity.[48,49] In the next few years, we expect to see a broader application of linear array-based PAT systems.

Acknowledgment

Yuehang Wang and Ye Zhan contributed equally to this work. This study was supported in part by the Career Catalyst Research Grant from the Susan G. Komen Foundation (No. CCR17481211).

References

1. L. V. Wang, J. Yao, "A practical guide to photoacoustic tomography in the life sciences," *Nat. Methods* **13**(8), 627 (2016).
2. L. V. Wang, S. Hu, "Photoacoustic tomography: in vivo imaging from organelles to organs," *Science* **335**(6075), 1458–1462 (2012).
3. J. Xia, L. V. Wang, "Small-animal whole-body photoacoustic tomography: A review," *IEEE Trans. Biomed. Eng.* **61**(5), 1380–1389 (2013).
4. S. Manohar, D. Razansky, "Photonics, Photoacoustics: A historical review," *Adv. Opt.* **8**(4), 586–617 (2016).
5. J. Xia, J. Yao, L. V. Wang, "Photoacoustic tomography: Principles and advances," *Progress In Electromagnetics Research* **147**, 1–22 (2014).
6. M. Holotta *et al.*, "Photoacoustic tomography of ex vivo mouse hearts with myocardial infarction," *J. Biomed. Opt.* **16**(3), 036007 (2011).
7. M. R. Chatni *et al.*, "Tumor glucose metabolism imaged in vivo in small animals with whole-body photoacoustic computed tomography," *J. Biomed. Opt.* **17**(7), 076012 (2012).
8. Y. Wang *et al.*, "A robust and secure palm vessel biometric sensing system based on photoacoustics," *IEEE Sensors J.* **18**(14), 5993–6000 (2018).
9. M. Nasiriavanaki *et al.*, "High-resolution photoacoustic tomography of resting-state functional connectivity in the mouse brain," *Proc. National Acad. Sci.* **111**(1), 21–26 (2014).
10. C. P. Favazza, L. V. Wang, L. A. Cornelius, "In vivo functional photoacoustic microscopy of cutaneous microvasculature in human skin," *J. Biomed. Opt.* **16**(2), 026004 (2011).
11. J. Xia *et al.*, "Calibration-free quantification of absolute oxygen saturation based on the dynamics of photoacoustic signals," *J. Opt. Lett.* **38**(15), 2800–2803 (2013).
12. Y. Zhou *et al.*, "Calibration-free in vivo transverse blood flowmetry based on cross correlation of slow time profiles from photoacoustic microscopy," *J. Opt. Lett.* **38**(19), 3882–3885 (2013).
13. R. A. Kruger *et al.*, "Dedicated 3D photoacoustic breast imaging," *Med. Phys.* **40**(11), 113301 (2013).
14. R. A. Kruger *et al.*, "Photoacoustic angiography of the breast," *Med. Phys.* **37**(11), 6096–6100 (2010).
15. A. Garcia-Uribe *et al.*, "Dual-modality photoacoustic and ultrasound imaging system for noninvasive sentinel lymph node detection in patients with breast cancer," *Sci. Rep.* **5**, 15748 (2015).
16. J. Xia *et al.*, "Enhancement of photoacoustic tomography by ultrasonic computed tomography based on optical excitation of elements of a full-ring transducer array," *Opt. Lett.* **38**(16), 3140–3143 (2013).
17. J. Xia *et al.*, "Whole-body ring-shaped confocal photoacoustic computed tomography of small animals *in vivo*," *J. Biomed. Opt.* **17**(5), 050506 (2012).
18. D. Wang *et al.*, "Deep tissue photoacoustic computed tomography with a fast and compact laser system," *Biomed. Opt. Exp.* **8**(1), 112–123 (2017).
19. L. Song *et al.*, "Fast 3-D dark-field reflection-mode photoacoustic microscopy *in vivo* with a 30-MHz ultrasound linear array," *J. Biomed. Opt.* **13**(5), 054028 (2008).

20. G. Li *et al.*, "Multiview Hilbert transformation for full-view photoacoustic computed tomography using a linear array," *J. Biomed. Opt.* **20**(6), 066010–066010 (2015).
21. G. Li *et al.*, "Tripling the detection view of high-frequency linear-array-based photoacoustic computed tomography by using two planar acoustic reflectors," *Quantitat. Imag. Med. Surg.* **5**(1), 57 (2015).
22. M. Yang *et al.*, "Photoacoustic/ultrasound dual imaging of human thyroid cancers: An initial clinical study," *Biomed. Opt. Exp.* **8**(7), 3449–3457 (2017).
23. M. H. Xu and L. V. Wang, "Analytic explanation of spatial resolution related to bandwidth and detector aperture size in thermoacoustic or photoacoustic reconstruction". *Physical Review E* **67**(5), 15 (2003).
24. C. Li, L. V. Wang, "High-numerical-aperture-based virtual point detectors for photoacoustic tomography," *Appl. Phys. Lett.* **93**(3), 033902 (2008).
25. L. V. Wang, "Tutorial on photoacoustic microscopy and computed tomography," *IEEE J. Select. Top. Quantum Electron.* **14**(1), 171–179 (2008).
26. M. Xu, L. V. Wang, "Universal back-projection algorithm for photoacoustic computed tomography," *Phys. Rev. E* **71**(1), 016706 (2005).
27. M. Li *et al.*, "Linear array-based real-time photoacoustic imaging system with a compact coaxial excitation handheld probe for noninvasive sentinel lymph node mapping," *Biomed. Opt. Exp.* **9**(4) 1408–1422 (2018).
28. J. Gateau *et al.*, "Three-dimensional optoacoustic tomography using a conventional ultrasound linear detector array: Whole-body tomographic system for small animals," *Med. Phys.* **40**(1), 013302 (2013).
29. J. Gateau *et al.*, "Single-side access, isotropic resolution, and multispectral three-dimensional photoacoustic imaging with rotate-translate scanning of ultrasonic detector array," *J. Biomed. Opt.* **20**(5), 056004–056004 (2015).
30. M. Schwarz, A. Buehler, V. Ntziachristos, "Isotropic high resolution optoacoustic imaging with linear detector arrays in bi-directional scanning," *J. Biophoton.* **8**(1–2), 60–70 (2015).
31. G. Li *et al.*, "Isotropic-resolution linear-array-based photoacoustic computed tomography through inverse Radon transform. in Photons Plus Ultrasound: Imaging and Sensing 2015," *Int. Soc. Opt. Photon.* **9323**, 93230I (2015).
32. Y. Wang *et al.*, "Slit-enabled linear-array photoacoustic tomography with near isotropic spatial resolution in three dimensions," *Opt. Lett.* **41**(1), 127–130 (2016).
33. Y. Wang *et al.*, "Second generation slit-based photoacoustic tomography system for vascular imaging in human," *J. Biophoton.* **10**(6–7), 799–804 (2017).
34. J. Xia *et al.*, "Three-dimensional photoacoustic tomography based on the focal-line concept," *J. Biomed. Opt.* **16**(9), 090505 (2011).
35. D. Wang *et al.*, "Coherent-weighted three-dimensional image reconstruction in linear-array-based photoacoustic tomography," *Biomed. Opt. Exp.* **7**(5), 1957–1965 (2016).
36. A. Alshaya *et al.*, Elevation resolution enhancement in 3D photoacoustic imaging using FDMAS beamforming, in *2017 IEEE Int. Ultrasonics Symp. (IUS)*, IEEE (2017), pp. 1–4.
37. L. Zhou *et al.*, "The detection and quantification of retinopathy using digital angiograms," *IEEE Trans. Med. Imag.* **13**, 619–626 (1994).
38. J. Gateau *et al.*, "Three-dimensional optoacoustic tomography using a conventional ultrasound linear detector array: Whole-body tomographic system for small animals," *J. Biomed. Opt.* **40**(1), 013302 (2013).
39. G. Wang *et al.*, "Simulation of light delivery for photoacoustic breast imaging using the handheld probe," *Chin. Opt. Lett.* **12**(5), 051703 (2014).
40. K. Sivasubramanian *et al.*, "Optimizing light delivery through fiber bundle in photoacoustic imaging with clinical ultrasound system: Monte Carlo simulation and experimental validation," *J. Biomed. Opt.* **22**(4), 041008 (2016).
41. Y.-H. Liu *et al.*, "A handheld real-time photoacoustic imaging system for animal neurological disease models: from simulation to realization," *Sensors* **18**(11), 4081 (2018).
42. G. S. Sangha, N. J. Hale, C. J. Goergen, "Adjustable photoacoustic tomography probe improves light delivery and image quality," *Photoacoustics* **12**, 6–13 (2018).
43. L. G. Montilla *et al.*, "Real-time photoacoustic and ultrasound imaging: A simple solution for clinical ultrasound systems with linear arrays," *Phys. Med.* **58**(1), N1 (2012).
44. Y.-J. Lee *et al.*, "Photoacoustic imaging probe for detecting lymph nodes and spreading of cancer at various depths," *J. Biomed. Opt.* **22**(9), 091513 (2017).
45. Y. Bai *et al.*, "Compact and low-cost handheld quasibright-field linear-array probe design in photoacoustic computed tomography," *J. Biomed. Opt.* **23**(12), 121606 (2018).
46. M. Li, C. Liu, L. Song, A novel compact linear-array based photoacoustic handheld probe towards clinical translation for sentinel lymph node mapping, in *Int. Conf. Biomedical and Health Informatics* (Springer, 2015).

47. Y. Wang *et al.*, "Optimizing the light delivery of linear-array-based photoacoustic systems by double acoustic reflectors," *Sci. Rep.* **8**(1), 13004 (2018).
48. Y. Zhu *et al.*, "Light emitting diodes based photoacoustic imaging and potential clinical applications," *Sci Rep.* **8**(1), 9885 (2018).
49. A. Fatima *et al.*, "Review of cost reduction methods in photoacoustic computed tomography," *Photoacoustics* **15**, 100137 (2019).